tion to a difference in the crystallization rates of the two polymers. The different crystallization rates were, in turn, attributed to a difference in the molecular weights of their samples. However, the difference in melting points of PED and PEH is undoubtedly the major cause of the different crystallization rates of our polymers. This is demonstrated by the fact that the crystallization rates of PED and PEH were virtually identical when compared at equal undercoolings. Moreover, molecular weight has a negligible effect on melting temperature at high molecular weight levels. Consequently, the minor difference in molecular weights of our PEH and PED samples cannot be the cause of the observed difference in melting temperatures.

Acknowledgments. We wish to acknowledge helpful discussions with Dr. D. K. Carpenter, Dr. J. J. McAplin, and Dr. C. S. Speed. Experimental data were obtained by J. O. Brewer, S. H. Killian, H. Kinsey, and Dr. S. H. Hastings.

Dilute-Solution Theory of Polymer Crystal Growth. Some Thermodynamic and Predictive Aspects for Polyethylene[1a]

Isaac C. Sanchez[1b] and Edmund A. DiMarzio*

Institute for Materials Research, National Bureau of Standards, Washington, D. C. 20234. *Received March 12, 1971*

ABSTRACT: The kinetic theory of polymer crystallization from dilute solution is applied to the system polyethylene–xylene. Prerequisite free energy driving forces are derived for crystallization from solution. These naturally depend on bulk thermodynamic properties and three thermodynamic potentials are derived depending on what melt and crystalline properties are assumed. The commonly used $\Delta H\Delta T/T_m^0$ expression is shown to be an upper bound for all materials and a more accurate expression descriptive of polyethylene is used in the actual calculations. Growth rate and lamella thickness are computed as functions of undercooling, concentration, and molecular weight. It is found that the growth rate varies roughly as concentration raised to a power, the value of the power being a function of both molecular weight and temperature. The isothermal lamella thickness increases only slightly with decreasing molecular weight and is even less dependent on concentration. The isothermal growth rate as a function of molecular weight exhibits a broad maximum. An analysis of the temperature dependence of the growth rate is made in terms of classical nucleation theory using calculations of the present theory as data points. This leads to the concept of an apparent $\sigma\sigma_e$ which is seen to vary as a function of molecular weight. The theory makes definitive, as yet unverified, predictions which can be tested experimentally.

I. Introduction

In a preceding paper,[2] hereafter referred to as I, a kinetic theory of polymer crystallization from dilute solution was developed. An interesting hypothesis of this theory is the postulated "self-nucleating" mechanism.[3] Cilia or dangling chain ends, which may be very long, are generated during the course of crystal growth; a very small fraction of these cilia participate in nucleating new growth strips (fold planes) on the crystal face and thus the crystal is quite capable of propagating itself without the benefit of external nucleating species (solution molecules). For a small-molecule nucleation theory, we would expect solution molecules to be the only nucleating species. If the self-nucleating mechanism predominates in dilute-solution crystallization of chain molecules as we suspect, then an anomalous dependence of crystal growth rates on polymer concentration can be anticipated. This topic is discussed in detail in section IIIC.

Two models were considered in I which describe the crystallization of chain molecules of finite length by regular chain folding. Both models can be characterized as "fractional stem rejection" models, since it is assumed that a fractional stem at the end of a folding chain is rejected by the crystal. Fractional stem incorporation causes defects in the crystal, and recent experimental evidence[4] suggests that most chain ends are found outside of the crystal. This assumption can be tested experimentally, as will be shown in section IIID, since the predicted temperature variation of the crystal growth rate should depend on whether or not chain ends are incorporated into the crystal.

In discussing the various predictive aspects of the kinetic theory obtained in I, we will specifically apply the theory to polyethylene (PE) dissolved in xylene.

II. Thermodynamics of Polymer Crystallization

The theory of polymer crystallization from solution requires a knowledge of the free energy difference between the undercooled solution and the equilibrium crystal. The free energy difference in turn is a sensitive function of the melting temperature of the crystalline polymer. The equilibrium melting temperature T_m^0 may be defined as that temperature at which pure *liquid* polymer is in thermal equilibrium with a large crystal—a crystal large enough that surface effects are negligible and one having an equilibrium number of defects. Presumably, the equilibrium crystal is an extended-chain crystal. Similarly, the equilibrium dissolution (melting) temperature T_d^0 may be defined as that temperature at which *polymer solution* is in equilibrium with the equilibrium crystal. Both T_m^0 and T_d^0 depend on the molecular weight of the polymer.

Denoting the molar free energy (chemical potential) of the monomer unit in the crystalline phase and in the pure liquid

(1) (a) Contribution of the National Bureau of Standards, not subject to copyright; (b) NRC–NAS Postdoctoral Research Associate, 1969–1971.

(2) I. C. Sanchez and E. A. DiMarzio, *J. Chem. Phys.*, **55**, 893 (1971).

(3) I. C. Sanchez and E. A. DiMarzio, *Bull. Amer. Phys. Soc.*, **15**, 377 (1970).

(4) A. Keller and D. J. Priest, *J. Macromol. Sci., Phys.*, **2**, 479 (1968).

polymer as μ_u^c and μ_u^0, respectively, the condition of equilibrium at a given pressure is expressed as

$$\mu_u^0 - \mu_u^c = \Delta H_u(T_m^0) - T_m^0 \Delta S_u(T_m^0) = 0 \quad (2.1)$$

where $\Delta H_u(T_m^0)$ is the heat of fusion and $\Delta S_u(T_m^0)$ is the entropy of fusion per mole of monomer at the melting temperature T_m^0. The condition of equilibrium in solution is

$$\mu_u^c = \mu_u = \mu_u^0 + RT_d^0 \ln a_u(T_d^0) \quad (2.2)$$

where μ_u is the chemical potential of the monomer unit in solution, $a_u(T_d^0)$ its activity, and R is the gas constant. In the next section various approximate forms of the free energy difference $\Delta G_u^0 \equiv \mu_u^0 - \mu_u^c > 0$ will be considered.

(A) Free Energy Difference between Liquid Polymer and Crystal. If it is assumed that both $\Delta H_u(T)$ and $\Delta S_u(T)$ are independent of temperature, then the difference in free energy per mole of monomer ΔG_u^0 between the undercooled liquid and crystal at temperature T is given by the well-known relation

$$\Delta G_{u1}^0 = \Delta H_u(T_m^0) - T\Delta S(T_m^0) = \frac{\Delta H_u(T_m^0)(T_m^0 - T)}{T_m^0} \quad (2.3)$$

where the additional subscript 1 on ΔG_u^0 denotes that this is the first approximation for ΔG_u^0 to be considered. By a general thermodynamic argument, it is shown in the Appendix that eq 2.3 is an *upper* bound of the actual free energy difference; the error inherent in eq 2.3 increases as the undercooling $\Delta T (= T_m^0 - T)$ increases.

If it is assumed that the entropy of the liquid S_l and of the crystal S_c are proportional to temperature ($S_l = k_1 T$, $S_c = k_2 T$), then a second approximation for ΔG_u^0 can be derived by utilizing the well-known thermodynamic equation $(\partial \Delta G/\partial T)_p = -\Delta S$ and the entropy of fusion relation at the melting temperature $\Delta S(T_m^0) = \Delta H(T_m^0)/T_m^0 = (k_1 - k_2)T_m^0$ to obtain

$$\Delta G_{u2}^0 = \int_T^{T_m^0} (k_1 - k_2)T' dT' = \frac{\Delta H_u(T_m^0)}{(T_m^0)^2} \int_T^{T_m^0} T' dT' = \Delta G_{u1}^0(1 + T/T_m^0)/2 \quad (2.4)$$

The assumption that S_l and S_c are proportional to temperature obtains for polyethylene (PE) in the usual crystallization temperature range. From extrapolated paraffin data, Broadhurst[5a] has found that S_l and S_c are approximately proportional to temperature from 200 to 400°K.

Other approximate expressions for ΔG_u^0 have been obtained,[6,7] but we will only consider one other approximation due to Hoffman[8] which is based on the assumption that the enthalpy of the liquid H_l and the enthalpy of the crystal H_c are linear functions of temperature (or, equivalently, the heat capacity difference ΔC_p between liquid and crystal is independent of temperature[6]). Omitting the details of the derivation, the result obtained when $H_l = H_c$ near the glass-transition temperature is

$$\Delta G_{u3}^0 = \frac{\Delta H_u(T_m^0)(T_m^0 - T)}{T_m^0}\left[\frac{T}{T_m^0}\right] = \Delta G_{u1}^0\left[\frac{T}{T_m^0}\right] \quad (2.5)$$

If $H_l = H_c$ near $T = 0$, an equation very similar to eq 2.4 obtains.[7]

(B) Free Energy Difference between Polymer Solution and Crystal. The difference in free energy ΔG_u per mole of monomer between polymer solution and crystal is given by

$$\Delta G_u = \mu_u - \mu_u^c = \mu_u^0 - \mu_u^c + RT \ln a_u(T)$$
$$\Delta G_u = \Delta G_u^0 + RT \ln a_u(T) \quad (2.6)$$

The activity $a_u(T)$ at temperature T is not known; however, $a_u(T_d^0)$ may be obtained, since the difference in free energy is zero at the equilibrium dissolution temperature, $\Delta G_u(T_d^0) = 0$.

$$\ln a_u(T_d^0) = -\Delta G_u^0(T_d^0)/RT_d^0 \quad (2.7)$$

If $a_u(T)$ is independent of temperature so that $a_u(T) = a_u(T_d^0)$, eq 2.7 can be used to obtain a useful approximation for ΔG_u. In general, the activity is temperature dependent; this temperature dependence can be examined by utilizing the Gibbs–Helmholtz equation

$$\frac{\partial}{\partial T}\left(\frac{\Delta G - \Delta G^0}{T}\right)\Big|_{P,n_1,n_u} = -\frac{\Delta H_m}{T^2} \quad (2.8)$$

and the relation

$$\Delta G - \Delta G^0 = n_u(\Delta G_u - \Delta G_u^0) + n_1(\mu_1 - \mu_1^0) \quad (2.9)$$

where ΔH_m is the heat of mixing solvent with *liquid* polymer, P is pressure, and n_1 and n_u are the numbers of moles of solvent and monomer, respectively. Differentiating eq 2.8 with respect to n_u (at constant P, T, n_1) and utilizing eq 2.6 yields

$$\frac{\partial \ln a_u}{\partial T}\Big|_{P,n_1,n_u} = -\frac{\overline{\Delta h_u}}{RT^2} \quad (2.10)$$

where $\overline{\Delta h_u}$ is the partial molar (per mole of monomer) heat of solution of liquid polymer and solvent.

$$\overline{\Delta h_u} = \frac{\partial \Delta H_m}{\partial n_u}\Big|_{P,T,n_1} \quad (2.11)$$

Equation 2.10 can be integrated to good approximation by replacing $\overline{\Delta h_u}$ by its average value in the temperature interval (T, T_d^0). The result is

$$\ln a_u(T) = \ln a_u(T_d^0) + (\overline{\Delta h_u}\Delta T/RTT_d^0) \quad (2.12)$$

where $\Delta T = T_d^0 - T$ is the degree of undercooling.

Hence, from eq 2.6, 2.7, and 2.12 we obtain the fundamental relation for the partial molar free energy difference $\Delta G_u(T)$ at a given temperature T.

$$\Delta G_u(T) = \Delta G_u^0(T) - \frac{T}{T_d^0}\Delta G_u^0(T_d^0) + \frac{\overline{\Delta h_u}\Delta T}{T_d^0} \quad (2.13)$$

Utilizing the three previously derived approximations for ΔG_u^0, we obtain three approximate relations for ΔG_u.

$$\Delta G_{u1} = [\Delta H_u(T_m^0) + \overline{\Delta h_u}]\frac{\Delta T}{T_d^0} \quad (2.14)$$

$$\Delta G_{u2} = \left[\frac{\Delta H_u(T_m^0)}{2}(1 + TT_d^0/(T_m^0)^2) + \overline{\Delta h_u}\right]\frac{\Delta T}{T_d^0} \quad (2.15)$$

$$\Delta G_{u3} = [\Delta H_u(T_m^0)(TT_d^0/(T_m^0)^2) + \overline{\Delta h_u}]\frac{\Delta T}{T_d^0} \quad (2.16)$$

If the partial molar heat of solution $\overline{\Delta h_u}$ is zero [athermal solution, which implies $a_u(T) = a_u(T_d^0)$] or if $\overline{\Delta h_u}$ is small compared to the heat of fusion $\Delta H_u(T_m^0)$, then these equations reduce to simpler forms. The simplified version ($\overline{\Delta h} = 0$) of eq 2.14 is the approximation usually seen in the literature.

(C) Dissolution Temperature for Lamellar Crystals. We

(5) M. Broadhurst, *J. Res. Nat. Bur. Stand., Sect. A*, **67**, 233 (1963).
(6) T. Suzuki and J. Kovacs, *Polym. J.*, **1**, 82 (1970).
(7) J. D. Hoffman and J. J. Weeks, *J. Chem. Phys.*, **37**, 1723 (1962).
(8) J. D. Hoffman, *J. Chem. Phys.*, **28**, 1192 (1958).

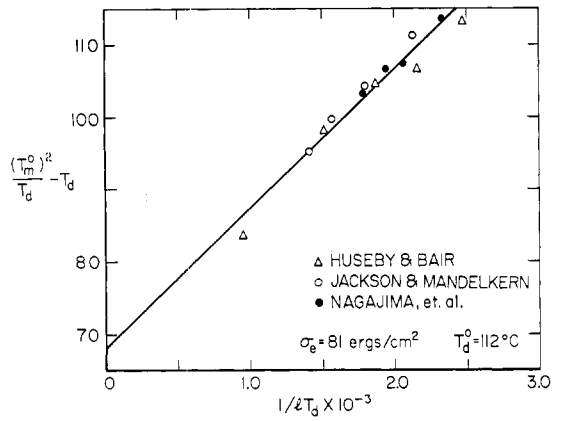

Figure 1. Linear least-squares analysis of dissolution temperature data for PE in xylene according to eq 2.19. The equilibrium melting temperature T_m^0 was taken to be 145°; however, the values of σ_e and T_d^0 obtained from the slope and intercept are not particularly sensitive to the value of T_m^0 employed (see text).

wish to derive expressions for the dissolution temperature T_d for thin, lamellar polymer crystals whose thickness l is much less than the lateral dimensions of the crystal. A lamellar crystal is in equilibrium with the solution when

$$\Delta G - 2\sigma_e/l = 0 \tag{2.17}$$

If the partial molar heat of solution $\overline{\Delta h}$ can be ignored, then the following simplified dissolution temperature equation is obtained from eq 2.14 and 2.17

$$1/T_d = (1/T_d^0) + (2\sigma_e/\Delta H)(1/lT_d) \tag{2.18}$$

while eq 2.15 and 2.17 yield

$$\frac{(T_m^0)^2}{T_d} - T_d = \frac{(T_m^0)^2}{T_d^0} - T_d^0 + \frac{4(T_m^0)^2\sigma_e}{\Delta H}\left(\frac{1}{lT_d}\right) \tag{2.19}$$

and eq 2.16 and 2.17 give

$$T_d = T_d^0 - (2(T_m^0)^2\sigma_e/\Delta H)(1/lT_d) \tag{2.20}$$

where ΔH is the heat of fusion in units of energy per unit volume of crystal formed at T_m^0. The above equations are valid even when σ_e is temperature dependent.

We have taken dissolution temperature data from the literature[9-11] for PE–xylene solutions and performed a linear least-squares analysis of these data as suggested by the functional forms of the above equations. In principle, values of σ_e and T_d^0 can be obtained from these data. A plot of these data according to eq 2.19 is shown in Figure 1 and a summary of the results for all three equations is given in Table I. Irrespective of the equation used in the analysis, the scatter of the data is not excessive. The values of σ_e and T_d^0 depend on the choice of T_m^0 for eq 2.19 and 2.20; $T_m^0 = 145°$ was used in preparing Table I. Letting $T_m^0 = 141°$ affects the calculated values of σ_e and T_d^0 in a negligible way (less than 2%). Note that the values of σ_e differ by as much as 25%, whereas the value of T_d^0 is essentially the same ($T_d^0 = 112°$) for all three equations. In each case T_d^0 was obtained by extrapolating the least-squares line to $1/lT_d = 0$ and σ_e from its slope (see Figure 1). Since these data represent various molecular weights (unfractioned Marlex,[9] 200,000 molecular weight fraction,[10] and ~20,000 molecular weight fraction[11]) it would appear that these kinds of experiments

(9) T. W. Huseby and H. E. Bair, *J. Appl. Phys.*, **39**, 4969 (1968).
(10) J. F. Jackson and L. Mandelkern, *Macromolecules*, **1**, 546 (1968).
(11) A. Nagajima, *et al.*, *Kolloid-Z. Z. Polym.*, **222**, 124 (1968).

TABLE I[a]

	Eq 2.18	Eq 2.19	Eq 2.20
σ_e, ergs/cm²	90.5	80.8	71.2
T_d^0, °C	112.4	112.1	111.9

[a] A linear least-squares analysis of dissolution temperature data (literature data) for dilute PE–xylene solutions yields the above values for the basal surface free energy σ_e and the equilibrium dissolution temperature T_d^0. In SI units, 1 erg/cm² = 0.001 J/m².

may not be sensitive enough to evaluate T_d^0 as a function of molecular weight. The extrapolated value of 112° found for T_d^0 represents some kind of average value for the molecular weight range studied. Moreover, if σ_e is temperature dependent, a straight-line extrapolation cannot be used to obtain T_d^0. An alternative approach for estimating T_d^0 will be discussed in the next section.

(D) The Equilibrium Dissolution Temperature. The equilibrium dissolution temperature T_d^0 for a given polymer–solvent system is a function of both concentration and molecular weight. However, it has been found that in dilute solutions, dissolution temperatures are only weakly dependent on concentration.[9,12,13] For a fixed concentration, the variation of T_d^0 with molecular weight is caused by two factors. The influence of both factors on T_d^0 can be seen from eq 2.7 and any one of the three approximations for ΔG_u^0. The following equations are obtained

$$T_d^0 = T_m^0[1/(1 - r)] \tag{2.21}$$

$$T_d^0 = T_m^0[r + (1 + r^2)^{1/2}] \tag{2.22}$$

$$T_d^0 = T_m^0(1 + r) \tag{2.23}$$

for ΔG_{u1}^0, ΔG_{u2}^0, and ΔG_{u3}^0, respectively, where $r = RT_m^0 \ln a_u(T_d^0)/\Delta H_u(T_m^0) \leqslant 0$. A knowledge of how T_d^0 varies with molecular weight is critically important to the understanding of fractionation effects that occur during crystallization from solution[12-14] and the variation of crystal growth rates with molecular weight. The above equations display that the variation of T_d^0 with molecular weight is caused by the molecular weight dependence of T_m^0 (which has been estimated for PE[4,15,16]) and the molecular weight dependence of a_u.[17] The activity a_u is a measure of the interaction (energetic and entropic) of polymer with solvent; in general, this interaction will be molecular weight dependent even at fixed concentration. In classical polymer solution theory, this is equivalent to saying that the χ interaction parameter is molecular weight dependent.

A method for determining the activity has been given by Pennings.[13] For dilute solutions his equation is

$$\ln a_u = \frac{V_u}{V_1}\left[\frac{\ln v_2 + 1}{x} - \left(\frac{1}{2} + \frac{V_1 A_2}{\bar{v}_2^2}\right)\right] \tag{2.24}$$

where A_2 is the second virial coefficient, $\bar{v}_2$ is the partial specific volume of the polymer, v_2 is the volume fraction of polymer,

(12) A. J. Pennings, *J. Polym. Sci., Part C*, **No. 16**, 1799 (1967); R. Koningsveld and A. J. Pennings, *Recl. Trav. Chim. Pays-Bas*, **83**, 552 (1964).
(13) A. J. Pennings in "Characterization of Macromolecular Structure," Publication No. 1573 of the National Academy of Science, Washington, D. C., 1968, p 214.
(14) W. R. Krigbaum and Q. A. Trementozzi, *J. Polym. Sci.*, **28**, 295 (1958).
(15) P. J. Flory and A. Vrij, *J. Amer. Chem. Soc.*, **85**, 3548 (1963).
(16) M. G. Broadhurst, *J. Res. Nat. Bur. Stand., Sect. A*, **70**, 481 (1966).
(17) A third possible factor is the MW dependence of the heat of fusion $\Delta H_u(T_m^0)$. For PE, this additional consideration is of no importance down to an MW of about 1000.[5a]

TABLE II[a]

MW	T_m^0, °C	T_d^0, °C Eq 2.21	Eq 2.22	Eq 2.23
1×10^4	140.0	100.8	98.9	96.6
2×10^4	142.7	107.4	106.0	104.2
5×10^4	144.4	112.4	111.2	110.0
1×10^5	144.9	114.5	113.4	112.1
5×10^5	145.4	116.9	116.0	114.9
1×10^6	145.4	117.4	116.5	115.4

[a] The equilibrium dissolution temperature T_d^0 for PE in xylene is calculated according to the Pennings formulation as a function of molecular weight using Flory–Vrij estimates of the equilibrium melting temperature T_m^0. The T_d^0 values obtained depend on the free energy of crystallization approximation that is employed.

V_1 is the molar volume of the solvent, V_u is the molar volume of the monomer unit, and x is the ratio of molar volumes of polymer and solvent. The second virial coefficient A_2 has been estimated from osmotic pressure measurements for PE in *p*-xylene as a function of molecular weight by Pennings[13] and by Krigbaum and Trementozzi.[14] The Pennings result is

$$A_2 = 1.47 \times 10^{-3} + 0.29/\sqrt{MW} \qquad (2.25)$$

From these equations estimates of T_d^0 as a function of MW can be determined for dilute solutions of PE in *p*-xylene; some selected values are given in Table II. The Flory–Vrij equation[15] was used to calculate T_m^0; other input data are $\Delta H_u = 980$ cal/mol, $V_1/\bar{v}_2^2 = 87.0$ g²/(ml mol), $V_1/V_u = 7.73$, and $v_2 = 10^{-4}$. Note that the dependence of T_d^0 on the approximate form of ΔG_u^0 employed is not too strong; as expected, this dependence weakens as $T_m^0 - T_d^0$ decreases. A comparison of the Flory–Vrij equation for T_m^0 and the Pennings equation, eq 2.22, for T_d^0 is given in Figure 2.

As noted by Pennings,[13] eq 2.25 for A_2 clearly breaks down for low molecular weights, causing the calculated values of T_d^0 to be too low. A possible explanation for the inadequacy of eq 2.25 for low molecular weight is that the temperature dependence of A_2 has been neglected (see ref 13 for more details on the experimental difficulties associated with determining this temperature dependence). The calculated value of 116.5° for T_d^0 for a 10^6 MW fraction is in good agreement

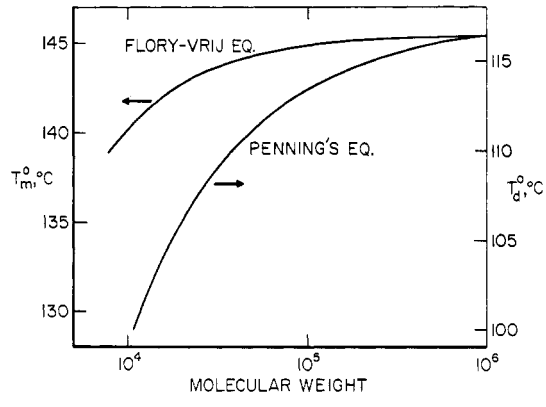

Figure 2. The Flory–Vrij estimate of the equilibrium melting temperature T_m^0 for PE is compared with the Pennings estimate of the equilibrium dissolution temperature T_d^0, eq 2.22, for dilute solutions of PE in *p*-xylene as a function of molecular weight. The figure shows that the calculated depression in the melting point, which is approximately 29° at a molecular weight of 10^6 and about 41° at a molecular weight of 10^4, is strongly dependent on the molecular weight of PE.

TABLE III
VALUES AND RANGES FOR THE PARAMETERS USED IN THE CALCULATIONS

Temperature, °C	84–94
Concentration	10^{-5}–10^{-2} (volume fraction)
Molecular weight	10^4–10^6
ΔH_u, cal/mol	980
T_m^0	Flory–Vrij values
T_d^0	Eq 2.26
ΔG_u	Eq 2.15 ($\overline{\Delta h} \ll \Delta H_u$)
a, Å	4.3
δ	1/4
DP/x = DP/N	7.73
σ, ergs/cm²	10
σ_e, ergs/cm²	120
f	3/4

with recent dissolution temperature experiments on high MW samples of stirrer-crystallized PE.[18] However, for a 1.2×10^4 fraction the calculated value of 102° does not compare favorably with the experimentally observed melting point of 106–108°.[19]

On the basis of the foregoing considerations, we have adopted the following semiempirical relation for T_d^0

$$T_d^0 = [T_m^0 - 29 + \tau_d^0]/2 \qquad (2.26)$$

where T_m^0 and τ_d^0 are the Flory–Vrij and Pennings estimates, respectively. On Figure 2 eq 2.26 would lie midway between the Flory–Vrij and Pennings curves. This equation also agrees favorably with the experimentally determined dissolution temperatures of C_{94} (MW $\simeq$ 1000).[19] If the Krigbaum and Trementozzi[14] values for the second virial coefficient A_2 are used, then the variation of T_d^0 with MW is similar to that of eq 2.26. However, the absolute magnitudes of the calculated dissolution temperatures are too high by about 6° over the entire MW range.

III. Results of the Kinetic Theory

(A) Constants, Parameters, and Variables. A listing of the constants, parameters, and variables with their ranges used in the calculations is given in Table III. The value of 10 ergs/cm² for σ is the usual value assigned to this surface free energy.[20–22] The value of 120 ergs/cm² for σ_e is an average value of σ_e in the aforementioned temperature range, although its precise numerical value is somewhat arbitrary. The only criterion used in selecting it was to choose a σ_e which would yield a crystal whose theoretical thickness l^* was close to the experimentally observed thickness l_{obsd} (more on this point in section IIIB).

We assume that the cross section of a crystal stem is square, with an area (*ca.* 18.5 Å²) one-half the area of the (001) cross section of the PE unit cell. This assumption will have no significant effect on the calculations. The intramolecular carbon–carbon bond distance projected on the *c* axis is 1.27 Å.

By definition, x is the ratio of the molar volume of polymer to solvent; N is the number of statistical elements in the chain. Pennings has estimated that the ratio of the degree of polymerization (DP) to x is 7.73 for PE in *p*-xylene.[13]

(18) A. M. Rijke and L. Mandelkern, *J. Polym. Sci, Part A-2*, **8**, 225 (1970).
(19) J. J. Weeks, unpublished data.
(20) D. Turnbull and R. L. Cormia, *J. Chem. Phys.*, **34**, 820 (1961).
(21) J. D. Hoffman, *SPE (Soc. Plast. Eng.) Trans.*, **4**, 315 (1964).
(22) C. Devoy, L. Mandelkern, and L. Bourland, *J. Polym. Sci., Part A-2*, **8**, 869 (1970).

In a Θ solvent Flory has estimated that DP/N = 10 for PE.[23] However, it has been assumed that DP/x = DP/N = 7.73, since this assumption has no significant effect on the calculations.

The total number of available chain configurations is reduced by a factor $1/(N-j)^{\delta}j^{\delta}$ when the jth element of the chain is attached to a crystal surface. For an ideal flexible chain (no excluded volume) and a large plane surface, $\delta = {}^1/_2$; for a real polymer chain and a realistic crystal surface, we have estimated in I that $\delta = {}^1/_4$.

Two models of polymer crystallization were considered in I. In the first model, primary cilia, which are formed in the initial attachment of the chain at a growth niche, were not allowed to reenter the crystal, whereas in the second model, primary cilia formed in one growth strip are allowed to reincorporate in the next growth strip. In both models cilia or solution molecules could act as nucleating agents. The net nucleation rates for these two models, denoted by S_{I} and S_{II}, are given by

$$S_{\mathrm{I}} = A_0(A_1 - B_2)/(A_1 - B_2 + B_1) \tag{3.1}$$

and

$$S_{\mathrm{II}} = A_0(A_1A_2 - B_2B_3)/[A_1A_2 - B_2B_3 + B_1(A_2 + B_2)] \tag{3.2}$$

where the rate constants A_0 and B_1 are the forward and backward nucleation rate constants for a nucleating species ν_0 stems in length, (A_1, B_2) is the rate constant pair associated with the addition of ν_1 stems of a solution molecule to an already nucleated growth strip, and the rate constants A_2 and B_3 describe the addition of ν_2 stems of a primary cilium (formed in a previous growth strip) to an adjacent growth strip. The nucleation rate S is proportional to N_0, the number of nucleation sites, which has been omitted from the above equations for convenience. The foregoing three pairs of rate constants can be expressed in terms of more fundamental rate constants associated with the attaching and detaching of individual crystal stems to a growth strip.

$$A_0 = \alpha_0{}^0(\alpha - \beta)/\{(\alpha - \beta) + \beta_1{}^0[1 - (\beta/\alpha)^{\nu_0 - 1}]\} \tag{3.3}$$

$$B_1 = A_0(\beta_1{}^0/\alpha_0{}^0)(\beta/\alpha)^{\nu_0 - 1} \tag{3.4}$$

$$A_1 = \alpha_0{}^1(\alpha - \beta)/\{(\alpha - \beta) + \beta_1{}^1[1 - (\beta/\alpha)^{\nu_1 - 1}]\} \tag{3.5}$$

$$B_2 = A_1(\beta_1{}^1/\alpha_0{}^1)(\beta/\alpha)^{\nu_1 - 1} \tag{3.6}$$

$$A_2 = (\alpha - \beta)/[1 - (\beta/\alpha)^{\nu_2}] \tag{3.7}$$

$$B_3 = A_2(\beta/\alpha)^{\nu_2} \tag{3.8}$$

The rate constant pairs ($\alpha_0{}^0$, $\beta_1{}^0$), ($\alpha_0{}^1$, $\beta_1{}^1$), and (α, β) are the forward and backward rate constants for a stem involved in nucleation, for the first stem of a solution molecule that adds to a growing strip, and for a stem adding to a growing strip that requires chain folding, respectively. These rate constants were determined in I and are given as follows

$$\alpha_0{}^1 = \exp(-F_{\mathrm{L}}/kT) \tag{3.9}$$

$$\beta_1{}^1 = \exp[-(a^2l\Delta G + F_{\mathrm{L}}/\nu)/kT] \tag{3.10}$$

$$\alpha = \exp(-2a^2\sigma_{\mathrm{e}}/kT) \tag{3.11}$$

$$\beta = \beta_1{}^1 \tag{3.12}$$

$$\alpha_0{}^0 = (\alpha_0{}^1/\beta_1{}^1)\exp(-2al\sigma/kT) \text{ (solution molecule)} \tag{3.13a}$$

$$\alpha_0{}^0 = (\alpha/\beta)\exp(-2al\sigma/kT) \text{ (cilium)} \tag{3.13b}$$

$$\beta_1{}^0 = 1 \tag{3.14}$$

where $F_{\mathrm{L}} = kT \ln (N^{2\delta}/v_2)$ is the localization free energy, l is the lamella or crystal thickness, $\nu = L/l$ is the number of stems per molecule, and L is the extended length of the chain. If f is the average fraction of a chain molecule that becomes incorporated into a growing strip and $(1 - f)$ is the average fraction of the chain that is left dangling out of the crystal as a primary cilium, then

$$\begin{aligned} \nu_0 &= [[fL/l]] \text{ (solution molecule)} \\ \nu_0 &= [[(1-f)L/l]] \text{ (cilium)} \end{aligned} \tag{3.15}$$

$$\nu_1 = [[fL/l]] \tag{3.16}$$

$$\nu_2 = [[(1-f)L/l]] \tag{3.17}$$

where the quantity $[[x]]$ means "largest integer less than or equal to x."

The calculations to be discussed here are based on a value of ${}^1/_4 = 1 - f$, but other calculations have been carried out for other values (${}^1/_6$ and ${}^1/_2$). The results are dependent on the average cilium length, but the main features of the growth rate behavior which we will describe later are not significantly different for any primary cilium length between ${}^1/_6$ and ${}^1/_2$. Once a choice is made, then it is assumed that every molecule that adds to the crystal forms a primary cilium of that chosen length.

The total nucleation rate S (for either model) can be expressed as a linear combination of the cilia nucleation rate S^{c} and the nucleation rate S^{s} for solution molecules

$$S = w_1S^{\mathrm{c}} + w_2S^{\mathrm{s}} \tag{3.18}$$

where w_1 and w_2 are weighting constants. It is difficult to make an *a priori* estimate of w_1 and w_2, although it is clear that w_1 is proportional to 1/MW, since the concentration of primary cilia (cilia per unit length of strip) produced in a growth strip varies as 1/MW. We have investigated S^{c} and S^{s} individually and have found that they behave qualitatively the same as a function of temperature and molecular weight, but there is a significant difference in their behavior as a function of polymer concentration in solution. This point will be discussed in section IIIC.

(B) Lamella Thickness. The nucleation rate $S = S(T, v_2, \mathrm{MW}, l)$ is a function of the crystallization temperature T, the concentration (volume fraction) v_2 of the polymer in solution, the molecular weight MW, and the thickness l of the lamella. When T, v_2, and MW are held constant, we find that *positive* nucleation rates exist over a range of lamella thicknesses; however, it is expected that the fast growing crystals are the experimentally observed crystals, which implies that we are interested in finding the thickness l^* that maximizes S (l^* satisfies the equation $\partial S/\partial l = 0$). Since S is in general unsymmetrical around l^* [it is usually skewed toward larger l, *i.e.*, $S(l^* + \delta l) \geq S(l^* - \delta l)$], the average thickness $\langle l \rangle$ of these crystallites will usually be larger than l^*. Previous kinetic theories[24-26] have identified $\langle l \rangle$ with the observed crystal thickness l_{obsd}. We have identified l^* with the lamella thickness. This choice will have little effect on the results of the theory, since $S(l^*)$ is only slightly greater than $S(\langle l \rangle)$.

(23) P. J. Flory, "Statistical Mechanics of Chain Molecules," Interscience, New York, N. Y., 1969, pp 326–327.

(24) J. I. Lauritzen, Jr., and J. D. Hoffman, *J. Res. Nat. Bur. Stand., Sect. A*, **64**, 73 (1960).

(25) F. C. Frank and M. Tosi, *Proc. Roy. Soc., Ser. A*, **263**, 323 (1961).

(26) F. Gornick and J. D. Hoffman, *Ind. Eng. Chem.*, **58**, 41 (1966).

Although no simple analytical expression can be obtained for l^*, we can place a lower bound on l^* since there exists a critical thickness l_c for which $S = 0$; if $l \leq l_c$, $S \leq 0$ and crystal growth does not occur. For a type II kinetic chain we see from eq 3.2 that $S_{II} = 0$ when $A_1A_2 - B_2B_3 = 0$, or

$$\ln (B_2B_3/A_1A_2) = 0 \tag{3.19a}$$

and from eq 3.5–3.8,

$$\ln (\beta_1{}^1/\alpha_0{}^1) + (\nu - 1) \ln (\beta/\alpha) = 0 \tag{3.19b}$$

where ν is the total number of stems per molecule. The ratios $\beta_1{}^1/\alpha_0{}^1$ and β/α are given by eq 3.9–3.12, thus

$$2(\nu - 1)\sigma_e - \nu l_c \Delta G = 0 \tag{3.19c}$$

Now, ν is dependent on l and is approximately given by $\nu = L/l$, where L is the extended length of the molecule; hence, eq 3.19c becomes

$$2(L/l_c - 1)\sigma_e - L\Delta G = 0 \tag{3.19d}$$

or

$$l_c \equiv l_c(L) = \frac{2\sigma_e/\Delta G}{1 + 2\sigma_e/L\Delta G} = \frac{l_c(\infty)}{1 + l_c(\infty)/L} \tag{3.19e}$$

The thickness $l_c(\infty)$ is defined as the minimum crystal thickness for an infinite chain which has the same equilibrium dissolution temperature $T_d{}^0$ as the chain of finite length L; thus $l_c(\infty)$ can vary with MW. The thickness $l_c(L)$ is the minimum thickness for which molecules of length L can form folded-chain crystals. Previous theories have identified l_c with $2\sigma_e/\Delta G$, but in the present theory l_c varies with the length or the molecular weight of the molecule; note that $l_c(L) \leq l_c(\infty) = 2\sigma_e/\Delta G$. The reason for this departure from the classical result is embodied in the inherent assumption that fractional stem lengths at either end of the molecular chain are rejected by the crystal. For this model, the incorporation of ν stems into the crystal results in the formation of $\nu - 1$ chain folds and, in general, two short cilia of length less than l_c. The assumption is that these short cilia compete with other molecules for position along the growth strip but they always lose out in the competition and are rejected.

For a type I growth strip, where primary cilia are not allowed to reincorporate into an adjacent growth strip (here one of the two rejected cilia is very long in contrast to the type II model where both cilia are fractional stems), the analog of eq 3.19c is given by

$$2a^2(\nu_1 - 1) - \nu_1 a^2 l_c \Delta G + \left(\frac{\nu - \nu_1}{\nu}\right) F_L = 0 \tag{3.20a}$$

where ν_1 is the average number of stems contributed by a molecule to the growth strip ($\nu_1 < \nu$) and F_L is the localization free energy previously defined. If f is the average fraction of the chain molecule that adds to the strip, then $\nu_1 \simeq fL/l$, $\nu \simeq L/l$, and eq 3.20a becomes

$$l_c(L) = \left[\frac{l_c(\infty)}{l_c(\infty) + [f - (1 - f)R]L}\right] fL \tag{3.20b}$$

where $R \equiv F_L/a^2L\Delta G$. Note that $a^2L\Delta G$ is the total free energy that would accompany the crystallization of a molecule of length L in extended-chain form (no folds); R is usually less than 0.4 for the range of variables (T, v_2, MW) considered.

In general, l_c given by eq 3.19c is less than or equal to that given by eq 3.20b; the difference is largest for very low MW and v_2, yet even then the difference is usually less than 25 Å. The two equations become identical for full incorporation of the molecule ($f = 1$) into the growth strips. Hereafter, eq 3.19c will be referred to when discussing l_c.

In section II we obtained a value for σ_e by analyzing dissolution temperature and crystal thickness data taken from the literature. Values of σ_e ranging from 70 to 90 ergs/cm^2 were obtained, depending on what dissolution temperature equation was used to analyze the data. Nevertheless, we have employed a $\sigma_e = 120$ ergs/cm^2 in all calculations that we will subsequently discuss. This choice of σ_e yields values of l^* in the temperature range 84–94° which are quite comparable with experimentally determined lamella thicknesses. There is reason to believe that a σ_e of say 80 ergs/cm^2 is inappropriate for a kinetic theory of crystallization in the aforementioned temperature range. The lamella surface formed under kinetic conditions and its associated σ_e (kinetic) may relax or "anneal without thickening"[27] with time. Hence, when a dissolution temperature measurement is made, the surface free energy that is measured may be more characteristic of an "equilibrium" surface with a σ_e(equil) < σ_e(kinetic). This view is consistent with the Lauritzen–Passaglia kinetic theory of polymer crystallization which predicts that a certain amount of surface roughness is to be expected.[27,28] The choice of $\sigma_e = 120$ ergs/cm^2 is in fair agreement with estimates of σ_e(kinetic) by Hoffman, *et al.*,[27] and Huseby and Bair[9] in the temperature range 84–94°.

An alternative explanation is that σ_e(kinetic) $\simeq$ 80 ergs/cm^2 and newly formed growth strips on the lamella face are thinner than l_{obsd}, but a thickening process sets in and the lamella gradually thickens to l_{obsd}.[7]

We should emphasize, however, that when values of $\sigma_e <$ 120 were used in the calculations the major conclusions of the theory concerning the temperature, concentration, and molecular weight dependence of the growth rate remained *unaltered.*

Another surprising aspect of the results is that $S_I{}^s(l) = S_{II}{}^s(l)$ and $S_I{}^c(l) = S_{II}{}^c(l)$ to a good approximation nearly over the entire range of T, v_2, and MW investigated. Only at low MW and v_2 and high T is there much difference in the nucleation rates. The inference is that reentrant growth does not significantly affect the nucleation rate. The numerical results that are displayed in Figures 3–10 are characteristic of either model of polymer crystallization. When appropriate, we have noted the difference in behavior of S^c and S^s.

In Figure 3 we have compared $l_c(\infty)$, $l_c(L)$, and l^* as a function of MW at $T = 84$ and 90°. It should be noticed that l^* tends to fall below $l_c(\infty)$ in the low MW region, but l^* remains above $l_c(L)$ for all MW. For lower concentrations l^* tends to increase slightly for a given MW, but the basic pattern of behavior as a function of MW remains the same. The drift toward thicker crystals at low MW is a direct consequence of $T_d{}^0$ decreasing with decreasing MW. Bair and Salovey[29] have measured lamella thickness as a function of MW from 2×10^4 to 2×10^6 for PE. They concluded that the lamella thickness was approximately constant (125 Å) in this MW range for a crystallization temperature of 85°. The predicted variation of l^* with MW in this MW range at 85° is not very large, and the Bair and Salovey results are not at variance with the present theory.

The temperature dependence of l^* is very similar to the temperature dependence of l^* in previous theories.[27] The characteristic feature of this behavior is that l^* decreases

(27) J. D. Hoffman, *et al.*, *Kolloid-Z. Z. Polym.*, **231**, 564 (1969).
(28) J. I. Lauritzen, Jr., and E. Passaglia, *J. Res. Nat. Bur. Stand., Sect. A*, **71**, 261 (1967).
(29) H. E. Bair and R. Salovey, *J. Macromol. Sci., Phys.*, **3**, 3 (1969).

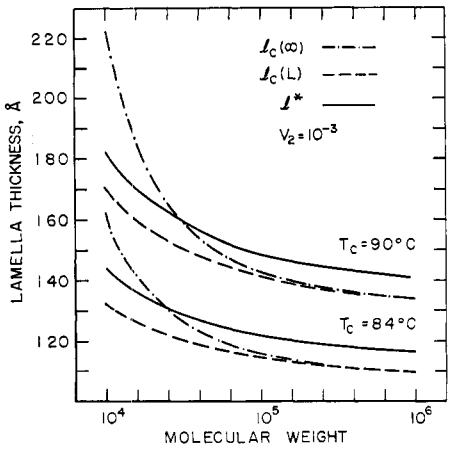

Figure 3. A comparison of lamellar thicknesses. The minimum stable (critical) thickness of a polymer of infinite length is $l_c(\infty)$ and is $l_c(L)$ for a polymer of finite extended length L. The observed lamellar thickness l^* (thickness which maximizes nucleation rate) can be less than the minimum thickness $l_c(\infty)$ of previous theories.

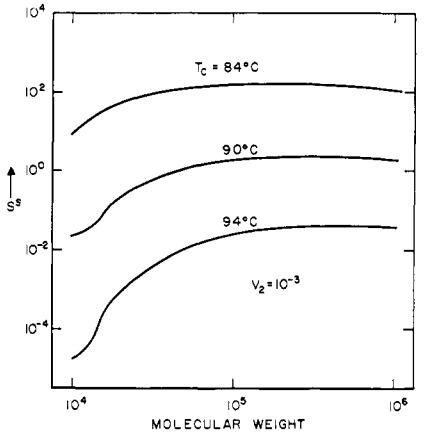

Figure 4. Isothermal nucleation rate for solution molecules S^s *vs.* molecular weight. Isotherms pass through a shallow maximum which shifts to higher molecular weights as the crystallization temperature increases.

with increased undercooling ΔT, but it finally reaches a minimum value and then begins to increase rapidly with any further increase in ΔT. In the present theory, the maximum crystal thickness is bounded at $L/2$ (one fold); this maximum thickness is approached as $\Delta T \rightarrow 0$ or when $\Delta T \rightarrow 2\sigma T_d^0/a\Delta H$ ($\Delta G \rightarrow 2\sigma/a$), which is about 60° for the parameters employed in this study. The critical undercooling $\Delta T_c = 2\sigma T_d^0/a\Delta H$ is the undercooling at which the free energy barrier opposing nucleation vanishes; moreover, the rate of nucleation approaches the rate at which the strip grows after nucleation ($\alpha_0^0 \rightarrow \alpha_0^1$). Under these conditions, the assertion that the growth of the crystal is strictly nucleation controlled is no longer valid, since the nucleation rate is comparable to the rate of postnucleated strip growth.

Interestingly enough, a choice of α_0^0 can be made so that l^* decreases monotonically with increasing ΔT without any blowup at some ΔT_c. This is accomplished by defining α_0^0 as

$$\alpha_0^0 = \exp(-2al\sigma/kT) \qquad (3.21)$$

rather than by eq 3.13. The bulk free energy term $a^2l\Delta G$ appears completely in β_1^0. With this apportionment of free energy, α_0^0 decreases slowly as ΔT increases (nucleation becomes increasingly more difficult), in contrast to eq 3.13 where α_0^0 increases with increasing ΔT so that the process of nucleation becomes easier. However, no theoretical justification has been found by us in support of this apportionment of free energy. The analysis presented in I based on sequential deposition of chain segments leads to eq 3.13 rather than to eq 3.21 for $\Delta G < 2\sigma/a$.

The question can be raised as to whether the free energy apportionment in eq 3.13 is an artifact of the steady-state approximation. The non-steady-state analysis by Longuet-Higgins[30] of a sequential process yields a free energy apportionment essentially identical with the steady-state apportionment in eq 3.13. His analysis of the kinetics of sequential desorption of a chain molecule on a surface with a strong attractive free energy is completely analogous to a nucleation step involving sequential deposition of chain segments on a surface with a repulsive free energy ($\Delta G < 2\sigma/a$).

We are led to the conclusion that the free energy apportionment of eq 3.13 is basically correct even under non-steady-state conditions. The predicted upswing, however, has never been observed experimentally. One explanation for this apparent disagreement is that other modes of crystal growth intervene before ΔT_c is reached.[25,31] Another explanation is that crystallization at high undercooling is nonisothermal; the concomitant rapid expulsion of the heat of fusion may place a limit on the actual undercooling that can be achieved experimentally. If this limit is less than ΔT_c, then the predicted upswing would never be observed. Our estimate of $\Delta T_c \simeq 60°$ is conservative; if σ is as strongly temperature dependent as has been proposed,[27] then ΔT_c is over 100° for PE.

(C) Molecular Weight and Concentration Dependence of the Nucleation Rates. In Figure 4 the variation of the nucleation rate S^s as a function of MW is shown at various crystallization temperatures. There are two characteristic features of these isotherms: the nucleation rate goes through a broad maximum as a function of MW, which is somewhat difficult to notice on the logarithmic scale of Figure 4; this maximum shifts to lower molecular weights as the crystallization tem-

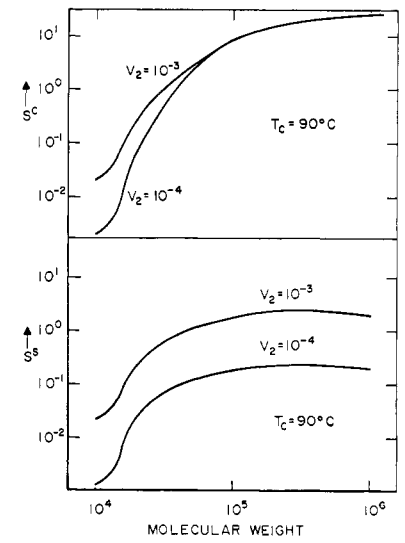

Figure 5. The relative effect of concentration on solution molecule and cilium isothermal nucleation rates, S^s and S^c, as a function of molecular weight.

(30) H. C. Longuet-Higgins, *Discuss. Faraday Soc.*, 25, 86 (1958).

(31) F. P. Price, *J. Chem. Phys.*, 35, 1884 (1961).

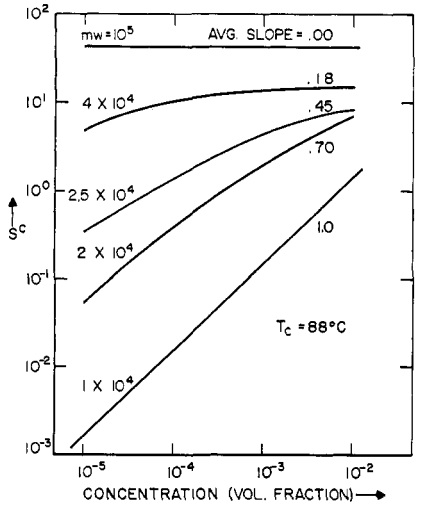

Figure 6. The effect of molecular weight on the concentration dependence of the isothermal cilia nucleation rate S^c. The concentration dependence decreases as the molecular weight increases.

perature is lowered. This type of growth rate behavior has not been reported for solution-grown crystals except qualitatively by Peterlin and Meinel.[32] They observed that an 85,000 MW fraction of PE crystallized more rapidly than either 10,000 or 300,000 MW samples at a fixed crystallization temperature. Jackson and Mandelkern[10] and Blundell and Keller[33] have also observed that high MW fractions crystallize faster than low MW fractions. Initially, the nucleation rate increases with MW because the undercooling ($T_d^0 - T$) is increasing. However, this effect of increased undercooling is opposed by the increase of the localization free energy F_L. These opposing effects produce the maxima in log S^s *vs.* log MW isotherms. The behavior of the cilia nucleation term S^c is slightly different; there are no maxima in log S^c *vs.* log MW isotherms of Figure 7, and S^c increases monotonically with MW. However, the inverse MW dependence of the weighting constant w_1 in eq 3.18 is sufficient to produce a broad maximum in a log ($w_1 S_c$) *vs.* log MW isotherm.

The influence of concentration on the nucleation rates can be seen in Figure 5. A tenfold increase in concentration has increased S^s approximately tenfold nearly over the entire MW range (the concentration dependence is slightly stronger

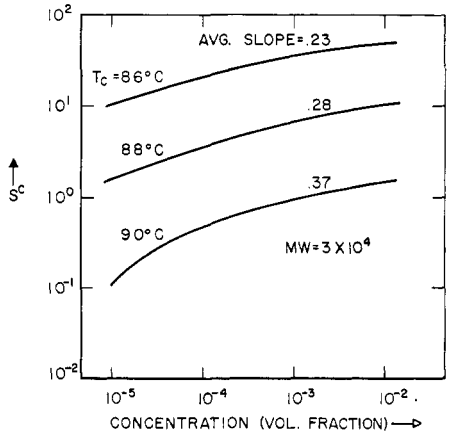

Figure 7. The effect of crystallization temperature T_c on the concentration dependence of the isothermal cilia nucleation rate S^c. The concentration dependence increases slightly as T_c increases.

(32) A. Peterlin and G. Meinel, *J. Appl. Phys.*, **35**, 3221 (1964).
(33) D. J. Blundell and A. Keller, *J. Polym. Sci., Part B*, **6**, 433 (1968).

for low MW's). The variation of S^c with concentration is strikingly different; in fact, above molecular weights of 10^5, S^c appears to exhibit no concentration dependence at all.

In Figures 6 and 7, the concentration dependence of S^c is examined more closely. The concentration dependence of S^c weakens as the molecular weight is increased at a fixed crystallization temperature or as the crystallization temperature is decreased at a fixed molecular weight. In general, S^c is proportional to the concentration raised to a power less than unity (fractional-order growth kinetics). In contrast, S^s is usually proportional to the concentration raised to the first power (first-order kinetics) except at very low molecular weights, where the concentration exponent tends to exceed unity.

The dependence of S^c and S^s on concentration in the limit of high MW is easily determined. From the defining relations for S_I and S_{II}, eq 3.1 and 3.2, and the rate constants A_0, B_1, A_1, etc., given by eq 3.3–3.8, we have

$$\lim_{MW\to\infty} S_I \text{ or } S_{II} = \lim_{MW\to\infty} A_0 = \frac{\alpha_0^0(\alpha - \beta)}{\beta_1^0 + (\alpha - \beta)} \quad (3.22)$$

Now, since $\beta_1^0 \gg \alpha$ or β, there obtains in the limit of high MW

$$S^s = \alpha_0^0(\alpha - \beta) \sim (v_2/MW^{2\delta})(1 - \beta/\alpha) \times \exp(-2al\sigma/kT) \quad (3.23)$$

and

$$S^c = \alpha_0^0(\alpha - \beta) = (\alpha/\beta)(\alpha - \beta)\exp(-2al\sigma/kT) \quad (3.24)$$

Thus, we see that for high molecular weights, S^s is proportional to v_2 and S^c is essentially independent of v_2.

In the limit of low MW, the analysis of the dependence of S^c and S^s on concentration is more approximate than in the limit of high MW. First, we must define what is meant by "low MW." Approximate expressions for S^s and S^c can be obtained if the nucleating species is less than five or six stems long ($\nu_0 < 6$). For a type I chain, we have

$$S_I = \frac{A_0(1 - B_2/A_1)}{B_1/A_1 + 1 - B_2/A_1} \quad (3.25)$$

To a crude approximation, in the limit of low MW we obtain

$$S^s \simeq A_1(A_0/B_1) \sim (v_2/MW^{2\delta})^{1+\nu_0/\nu} \quad (3.26)$$

and

$$S^c \simeq A_1(A_0/B_1) \sim (v_2/MW^{2\delta})^{1-\nu_0/\nu} \quad (3.27)$$

In the present study $\nu_0/\nu \simeq 1/4$. For a type II chain the concentration dependence is approximately the same. The enlightening aspect of eq 3.26 and 3.27, even though they are crude approximations, is that they show in the limit of low MW that S^s is proportional to concentration raised to a power greater than unity, whereas S^c is proportional to concentration raised to a power less than unity.

For a given MW, the production of primary cilia in a growth strip (number of cilia per unit length of growth strip) is independent of the polymer concentration. On this basis, one might expect that S^c would always be independent of polymer concentration irrespective of the MW of the polymer, but as Figure 6 and eq 3.27 illustrate, this is not the case. The physical explanation is simple. The efficiency of a nucleation event depends on how the nucleus grows; a certain amount of strip growth (stem addition) is required to stabilize the nucleus, otherwise the nucleus may "melt" off the crystal surface. If the nucleating species is very long, it is able to

stabilize itself by chain folding, but if it is short, say two or three stems long, then molecules from the solution are required to stabilize the nucleus. The availability of these solution molecules for stabilization, of course, depends on the concentration of the polymer in solution.

We can now understand why the concentration dependence of S^c tends to increase with increasing crystallization temperature as shown in Figure 7. At the high crystallization temperatures, l^* increases and the number of stems that a molecule can contribute to the growth strip is reduced; at the higher temperatures the "effective length or MW" of the molecule is reduced and thus, in accord with Figure 8, the concentration dependence tends to increase.

It was mentioned earlier that it is difficult to estimate *a priori* whether S^c and S^s contribute more or less equally to the total nucleation rate or whether one term dominates the other. It is possible to answer this question experimentally because of the fundamental difference in the concentration dependence of these terms. Blundell and Keller[38] have investigated the concentration dependence of the growth rate of PE single crystals from xylene solution; they found that the growth rate has a weak dependence on concentration (of the order of $v_2^{1/3}$). In addition, they also observed that the dependence increases slightly as the crystallization temperature is raised. This growth rate behavior is in good agreement with the predicted behavior of S^c. However, Blundell and Keller employed unfractioned polymer (Marlex 6009) in their study, which raises the question as to whether the experimental evidence supports a "self- nucleation" mechanism of crystal growth or if it is some manifestation of the MW fractionation that certainly must be occurring during crystallization. More experimental work, preferably with sharp MW fractions, is needed before any definite conclusions can be drawn.

(D) Temperature Dependence of the Nucleation Rate. According to classical nucleation theory[26] the nucleation rate S of monolayers on a surface is given by

$$S \sim \exp\left\{-\frac{2a\sigma}{kT}l_c(\infty)\right\} = \exp\left\{-\frac{4a\sigma\sigma_e}{kT\Delta G}\right\} \quad (3.28)$$

In the simplest approximation, the bulk free energy change ΔG is proportional to the undercooling ΔT (see eq 2.14); thus, a plot of ln S *vs.* $1/T\Delta T$ should be linear and the slope proportional to $\sigma\sigma_e$, which we refer to below as the "apparent $\sigma\sigma_e$." Some earlier nucleation theories of polymer crystallization can also be cast in the form of eq 3.28.[26] The nucleation rate, eq 3.1 or eq 3.2, in the present theory (for either S^s or S^c) can be approximately represented as

$$S \sim \exp\left\{-\frac{2a\sigma l_c(L)}{kT}\right\} = \exp\left\{-\frac{4a\sigma\sigma_e}{kT\Delta G(1 + l_c(\infty)/L)}\right\} \quad (3.29)$$

This approximate form contains most of the temperature dependence of the nucleation rate. Therefore, a plot of ln S *vs.* $1/T\Delta T$ is approximately linear (if it is assumed that ΔG is proportional to ΔT), with a slope proportional to $\sigma\sigma_e/(1 + l_c(\infty)/L)$; since $l_c(\infty)$ is a function of temperature, it is the average value of $l_c(\infty)$ in the given temperature range that is appropriate. In Figure 8 we have plotted the theoretical ln S^c *vs.* $1/T\Delta T$ and analyzed the slopes according to eq 3.28; *i.e.*, we assume the slope is equal to $4a\sigma\sigma_e T_d^0/k\Delta H$ and calculate an "apparent $\sigma\sigma_e$" as a function of MW. The $\sigma\sigma_e$ product calculated in this manner for S^c and S^s is shown in Figure 9; the actual $\sigma\sigma_e$ value used in all calculations was 1200 ergs^2/cm^4.

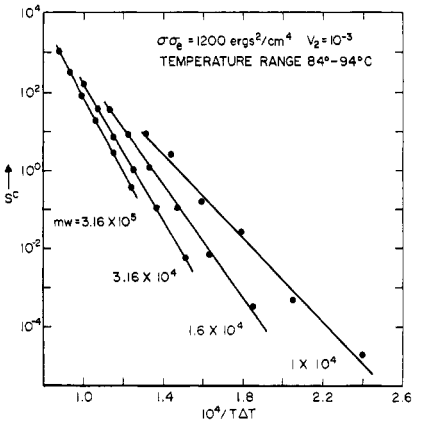

Figure 8. A plot of the cilia nucleation rate S^c *vs.* $1/T\Delta T$. The calculated values are shown and are at 2° intervals. Note that although the $\sigma\sigma_e$ product is held constant, the average slope of these curves decreases with decreasing molecular weight.

At high MW the apparent $\sigma\sigma_e$ tends to exceed by about 10% the actual value of 1200. The main cause of this difference is that eq 2.15 was used for the bulk free energy change in the calculations rather than the usual approximation, eq 2.14. At low molecular weights, the apparent $\sigma\sigma_e$ falls below 1200; the term $l_c(\infty)/L$ begins to contribute in eq 3.29 (for example, when MW = 12,000 the average value of $l_c(\infty)/L$ is about 0.2), which causes the reduction in the apparent $\sigma\sigma_e$. As discussed in section IIIB, the significance of this additional term $l_c(\infty)/L$ is that low MW crystals are able to grow at thicknesses less than the predicted classical value of $2\sigma_e/\Delta G$. This term arises because the simple approximation is made that fractional stems at the ends of the chain are rejected from the crystal and do not alter the nucleation kinetics.

The σ_e that enters the present theory represents the contribution to the surface free energy made by a chain fold. The surface free energy of a fully grown crystal will depend on the density of the cilia on the surface as well as the presence of chain folds.[21] Equation 3.29 has the same functional form as eq 3.28 if we define a new surface free energy σ_e' to be equal to $\sigma_e/(1 + l_1(\infty)/L)$. Cilia on the crystal surface have the effect of lowering the surface free energy of the crystal. Therefore, the values of σ_e obtained from melting

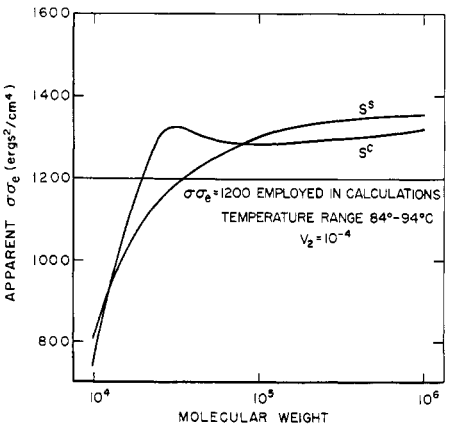

Figure 9. Apparent $\sigma\sigma_e$ *vs.* molecular weight. The present theory deviates from classical theory at low molecular weight because chain end group rejection is postulated, while the deviation at high molecular weight is caused by the use of an improved free energy of crystallization function.

point determinations (dry or wet crystals) as a function of MW would also be expected to follow the same trend as shown in Figure 9.

Alternatively, a model of crystal growth that can be considered is one in which fractional stems are always *incorporated.* This is equivalent to introducing defects into the crystal structure, and it is clear that the density of these defects would depend strongly on the MW of the polymer. Qualitatively, the defects can be accounted for by combining the defect energy and surface free energy and redefining a new surface free energy σ_e' which includes the defect energy. Thus $\sigma_e' \geq \sigma_e$, and

$$\lim_{MW \to \infty} \sigma_e' = \sigma_e \tag{3.30}$$

For this model, the apparent $\sigma\sigma_e$ would tend to *increase* with decreasing MW, in contrast with the behavior exhibited by a fractional stem rejection model as shown in Figure 9. If chain end rejection predominates as recent experiments suggest, then behavior more akin to Figure 9 can be expected.

(E) Growth Mode Diagram. Finally, eq 3.19e for $l_c(L)$ allows us to determine the *minimum* undercooling, ΔT_{min}, required for folded-chain crystal growth. For a chain of extended length L, the maximum possible thickness for a folded-chain crystal is $L/2$. Substituting $L/2$ into eq 3.19e and using eq 3.14 for ΔG, we obtain

$$\Delta T_{min} = (2\sigma_e/\Delta HL)T_d^0 \tag{3.31}$$

If crystallization occurs at undercooling less than ΔT_{min}, then extended-chain or some other type of nonfolded-chain crystal growth will take place. In nonfolded crystallization, we include crystals whose lamella thickness is less than L but greater than $L/2$. Figure 10 illustrates how ΔT_{min} varies with MW. In addition, some relative growth or nucleation rates for folded-chain crystal growth are shown. The usual experimental crystallization region falls between the 10^{-2} and 10^2 lines of constant growth rate.

IV. Summary

The thermodynamics of polymer crystallization from solution have been investigated. A fundamental equation for the partial molar free energy difference ΔG between crystal and solution has been obtained. This equation is a function of the free energy difference between crystal and melt, ΔG^0, the equilibrium dissolution temperature, T_d^0, and the partial molar free energy of mixing, $\overline{\Delta h}$, of solvent and liquid polymer. The usual approximation employed for ΔG^0 is shown to be an upper bound for the actual free energy change; other approximations are considered, and a good approximation for PE has been found. In addition, the influence of these various approximations on the determination of thermodynamic parameters from experimental data has been considered.

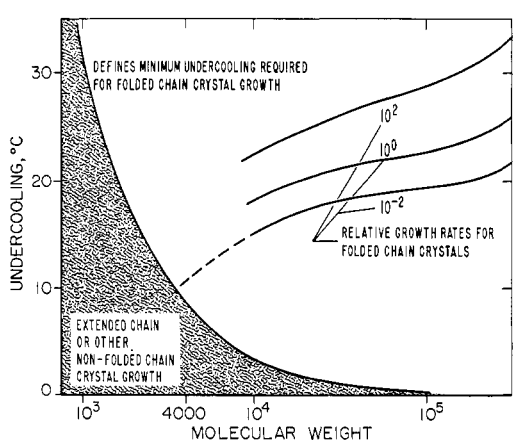

Figure 10. Growth mode diagram. Chain-folded crystallization does not occur in the stippled region. The usual experimental crystallization range where chain folding occurs is bounded by the 10^{-2} and 10^2 lines of constant nucleation rate.

Using PE in xylene as a model polymer–solvent system, the kinetic theory obtained in I has been utilized to calculate the growth rates (nucleation rates) of PE crystals as a function of MW, concentration, and crystallization temperature. As a function of MW, the growth rate at fixed concentration and temperature initially increases with increasing MW, but eventually passes through a broad maximum.

The concentration dependence of the growth rate depends on whether the nucleating species are solution molecules or cilia. In the former case, the growth rate is proportional to concentration (first order kinetics), while in the latter case the growth rate is proportional to concentration raised to a power less than unity (fractional order kinetics). The magnitude of the concentration exponent at a given crystallization temperature for self-nucleation decreases as the MW increases; at a given MW the exponent increases as the crystallization temperature increases. These definitive predictions concerning the concentration dependence of the growth rate may be used to test experimentally the validity of the self-nucleation mechanism. It should be borne in mind that the present theory is applicable only to sharp MW fractions; a paper dealing with the behavior of polydisperse systems is in preparation. Moreover, the theory is descriptive of nucleation-controlled crystal growth, which, from all experimental indications, appears to be characteristic of polymers crystallized from solution; self-propagating growth mechanisms (for example, screw dislocations) are not considered.

The assumption is made in the kinetic theory that a fractional stem at the end of a folding chain is rejected by the crystal. A consequence of this assumption is that low MW crystals are able to grow at thicknesses less than the predicted classical value of $l_c(\infty) = 2\sigma_e/\Delta G$. As a result, the predicted temperature dependence of the growth rate (the logarithm of the growth rate is approximately inversely proportional to the undercooling) of a "fractional stem rejection" model is different from that of a model where fractional stems are fully incorporated into the crystal. Because of this difference, the hypothesis of fractional stem rejection can be subjected to experimental test. Equation 3.28 is a valid representation of the nucleation rate for high molecular weights, but use of this equation for low MW polymers where end effects are important is, in general, incorrect. The specific model that is chosen (fractional stem rejection, fractional stem incorporation, etc.) will determine the specific form of eq 3.28 at low molecular weights. Equation 3.29 obtains for the rejection model.

A prescription for calculating nucleation rates and lamella thicknesses as a function of MW, concentration, and temperature is given as follows. First, values for the parameters of Table III for the polymer–solvent system in question are chosen. Next, either eq 3.1 or eq 3.2 is used to calculate the nucleation rate with the values for the rate constants given by eq 3.3–3.17. The lamella thickness l^* that maximizes S for fixed values of MW, concentration, and temperature is taken to be the crystal thickness and $S(l^*)$ the corresponding nucleation rate.

Appendix. Upper and Lower Bounds for the Bulk Free Energy of Fusion ΔG^0

At constant pressure, the following thermodynamic relations hold

$$dH_l = C_{p(l)}dT \tag{A.1}$$

$$dH_s = C_{p(s)}dT \tag{A.2}$$

where H is the enthalpy and C_p is the heat capacity at constant pressure; the subscript l refers to the liquid phase and the subscript s refers to the solid phase. Integration of eq A.1 and A.2 between T and T_m^0, followed by subtraction of one equation from the other yields

$$\Delta H(T_m^0) - \Delta H(T) = \int_T^{T_m^0} \Delta C_p dT' \tag{A.3}$$

where ΔH is the heat of fusion and $\Delta C_p = C_{p(l)} - C_{p(s)} > 0$.

From the thermodynamic relation

$$dS = (C_p/T)dT \tag{A.4}$$

we also obtain the following relations for the entropy of fusion, ΔS.

$$\Delta S(T_m^0) - \Delta S(T) = \int_T^{T_m^0} (\Delta C_p/T')dT' \tag{A.5}$$

Now, for $T < T_m^0$

$$T\Delta S(T_m^0) - T\Delta S(T) = \int_T^{T_m^0} (T/T')\Delta C_p dT' \leq \int_T^{T_m^0} \Delta C_p dT' = \Delta H(T_m^0) - \Delta H(T)$$

or

$$\Delta H(T) - T\Delta S(T) \leq \Delta H(T_m^0) - T\Delta S(T_m^0)$$

$$\Delta G^0 \leq \frac{\Delta H(T_m^0)(T_m^0 - T)}{T_m^0} \tag{A.6}$$

where ΔG^0 is the free energy of fusion. In deriving the inequality A.6 we have made use of the relation $\Delta S(T_m^0) = \Delta H(T_m^0)/T_m^0$. The right-hand side of the inequality A.6 is the usual approximation used to represent the free energy of fusion.

From the inequality

$$\int_T^{T_m^0} (T_m^0/T')\Delta C_p dT' \geq \int_T^{T_m^0} \Delta C_p dT' \tag{A.7}$$

we can obtain a lower bound for $\Delta G^0(T)$

$$T_m^0[\Delta S(T_m^0) - \Delta S(T)] \geq \Delta H(T_m^0) - \Delta H(T) \tag{A.8}$$

The inequality A.8 immediately implies that

$$\Delta S(T) \leq \Delta H(T)/T_m^0 \tag{A.9}$$

Therefore

$$\Delta H(T) - T\Delta S(T) \geq \Delta H(T) - (T/T_m^0)\Delta H(T)$$

$$\Delta G^0 \geq \frac{\Delta H(T)\Delta T}{T_m^0} \tag{A.10}$$

In summary, then

$$\Delta H(T)\Delta T/T_m^0 \leq \Delta G^0 \leq \Delta H(T_m^0)\,\Delta T/T_m^0 \tag{A.11}$$

If it is assumed that $\Delta G^0 = \Delta H(T_m^0)\Delta T/T_m^0$, then the maximum error, E_{max}, inherent in this approximation is given by

$$E_{max} = \frac{[\Delta H(T_m^0) - \Delta H(T)]\Delta T/T_m^0}{\Delta H(T_m^0)\Delta T/T_m^0} =$$

$$1 - \Delta H(T)/\Delta H(T_m^0) \simeq \frac{\Delta C_p \Delta T}{\Delta H(T_m^0)} \tag{A.12}$$

For PE, $\Delta C_p \simeq 1$ cal/(mol °K), $\Delta H(T_m^0) \simeq 1000$ cal/mol, and $E_{max} \simeq \Delta T/1000$.